$^{13}C-^{13}C$ Spin−Spin Coupling Tensors in Benzene As Determined Experimentally by Liquid Crystal NMR and Theoretically by *ab Initio* Calculations

Jaakko Kaski, Juha Vaara, and Jukka Jokisaari*

Contribution from the NMR Research Group, Department of Physical Sciences, University of Oulu, FIN-90571 Oulu, Finland

Received April 17, 1996[⊗]

Abstract: This study reports experimentally and theoretically (*ab initio*) determined indirect CC spin−spin coupling tensors $^{n}\mathbf{J}_{CC}$ in benzene. The CC spin−spin coupling constants $^{n}J_{CC}$ between the *ortho, meta*, and *para* ($n = 1$, 2, and 3) positioned carbons were experimentally determined in two ways: firstly by utilizing the $^{2}H/^{1}H$ isotope effect on the carbon shieldings in neat monodeuteriobenzene and recording the ^{13}C satellite spectrum in a ^{1}H-decoupled ^{13}C NMR spectrum, and secondly by recording the ^{13}C NMR spectrum of fully ^{13}C-enriched benzene ($^{13}C_6H_6$) and carrying out its complete analysis. The anisotropies of the corresponding coupling tensors, $\Delta^{n}J_{CC}$, were resolved experimentally by liquid crystal ^{1}H and ^{13}C NMR using dipolar couplings corrected for both harmonic vibrations and deformations. The results obtained in three thermotropic liquid crystal solvents are in good mutual agreement, indicating the reliability of the determinations. The anisotropy of the *ortho, meta*, and *para* CC indirect couplings are ca. +17, −4, and +9 Hz, respectively. Also, the signs of the coupling constants are unambiguously determined. The *ab initio* calculations were performed using multiconfiguration self-consistent field linear response theory with both single-reference and multireference wave functions. The results confirm the signs of the experimental anisotropies in all cases. The magnitude of the *ortho* coupling anisotropy is excellently reproduced, but the anisotropies are somewhat overestimated in the two other theoretical coupling tensors. The importance of the different physical contributions to the couplings and anisotropies is discussed.

Introduction

Nuclear magnetic resonance (NMR) spectra of solute molecules in liquid crystal phases or solid state samples display fine structure due to anisotropic *D* couplings, providing information on molecular geometry and orientation. In the experimental spectra, the direct dipolar coupling appears combined with a contribution of the indirect spin−spin coupling tensor, **J**.[1] The spin−spin coupling tensors are of fundamental significance in NMR spectroscopy, as they contain information on the electronic structure of the species. Progress in the application of liquid crystal NMR spectroscopy (LC NMR), in particular the development of models for taking into account the correlation between molecular vibrational and reorientational motions,[2] has rendered the investigations of indirect spin−spin coupling tensors even with small anisotropy, ΔJ, possible,[3] unlike solid state NMR.[1b]

Independent determination of the **J** tensors by *ab initio* electronic structure calculations has also emerged as a feasible method in small molecules due to the rapid development of computer hardware and recent advances in the applicable theoretical methodologies: the multiconfiguration self-consistent field (MCSCF),[4] coupled cluster singles and doubles (CCSD),[5] density-functional (DFT),[6] different polarization propagator,[7] and equation-of-motion[8] theories have displayed successful applications.

Reliable experimental determination as well as theoretical calculations of spin−spin coupling tensors are extremely demanding tasks. When applying LC NMR, one has to measure with good accuracy small differences between experimental *D* couplings and ones calculated from the molecular structure and orientation tensor. This definitely requires consideration of molecular vibrations,[9,10] as experimental *D* couplings are averages over vibrational motion, and the so-called deformational effects arising from the anisotropic forces experienced by solute molecules in a liquid-crystalline environment.[2] In addition to the need to have relatively large ΔJ values as compared to the corresponding direct couplings, the solid state method, in turn, requires preferentially large single crystal samples, although a few analyses of powder spectra arising from isolated spin pairs have been published (see ref 1b and references therein).

Indirect spin−spin coupling poses heavy requirements on computer time, the basis sets used, and the treatment of electron correlation in *ab initio* calculations. This is because of the existence of several contributing physical mechanisms:[1] the dia-

* To whom correspondence should be addressed. Fax: +358-81-553 1287. E-mail: Jukka.Jokisaari@oulu.fi.

[⊗] Abstract published in *Advance ACS Abstracts,* August 15, 1996.

(1) (a) Lounila, J.; Jokisaari, J. *Prog. Nucl. Magn. Reson. Spectrosc.* **1982**, *15*, 249−90. (b) Wasylishen, R. E. *Encyclopedia of NMR Spectroscopy*; John Wiley & Sons: New York, 1996; Vol. 2, pp 1685−95.

(2) (a) Lounila, J.; Diehl, P. *J. Magn. Reson.* **1984**, *56*, 254−61. (b) Lounila, J.; Diehl, P. *Mol. Phys.* **1984**, *52*, 827−45. (c) Lounila, J. *Ibid.* **1986**, *58*, 897−918.

(3) Jokisaari, J. *Encyclopedia of NMR Spectroscopy*; John Wiley & Sons: New York, 1996; Vol. 2, pp 839−48.

(4) Vahtras, O.; Ågren, H.; Jørgensen, P.; Jensen, H. J. Aa.; Padkjær, S. B.; Helgaker, T. *J. Chem. Phys.* **1992**, *96*, 6120−5.

(5) Sekino, H.; Bartlett, R. J. *J. Chem. Phys.* **1986**, *85*, 3945−9. Salter, E. A.; Sekino, H.; Bartlett, R. J. *Ibid.* **1987**, *87*, 502−9.

(6) (a) Malkin, V. G.; Malkina, O. L.; Salahub, D. R. *Chem. Phys. Lett.* **1994**, *221*, 91−9. (b) Dickson, R. M.; Ziegler, T. *J. Phys. Chem.* **1996**, *100*, 5286−90.

(7) (a) Geertsen, J.; Oddershede, J. *Chem. Phys.* **1987**, *104*, 67−72. (b) Geertsen J.; Oddershede, J.; Scuseria, G. E. *J. Chem. Phys.* **1987**, *87*, 2138−42.

(8) (a) Galasso, V. *J. Chem. Phys.* **1985**, *82*, 899−904. (b) Galasso, V.; Fronzoni, G. *Ibid.* **1986**, *84*, 3215−23.

(9) Sýkora, S.; Vogt, J.; Bösiger, H.; Diehl, P. *J. Magn. Reson.* **1979**, *36*, 53−60.

(10) Lounila, J.; Wasser, R.; Diehl, P. *Mol. Phys.* **1987**, *62*, 19−31.

S0002-7863(96)01263-2 CCC: $12.00 © 1996 American Chemical Society

and paramagnetic spin−orbit interaction terms (DSO and PSO), the Fermi contact term (FC), and the spin−dipole term (SD) all appear in the isotropic coupling constant J, *i.e.*, the trace of the coupling tensor. ΔJ, in turn, is affected by contributions from DSO, PSO, SD, and the cross-term of the SD and FC mechanisms (SD/FC). Often FC dominates J, but the insignificance of the other contributions cannot be known *a priori*,[11] even less so for the anisotropy ΔJ. Three of the contributions (FC, SD, and SD/FC) involve triplet excitation operators which may render restricted Hartree−Fock (or second-order many-body perturbation theory, MP2) results meaningless. Additionally, an excellent description of the electron density at the nuclei is needed for the FC contribution.

The case of aromatic CC couplings is crucial for structure determinations in liquid-crystalline and biomolecular systems. Most molecules that display thermotropic liquid-crystalline properties include one or more benzene rings. Recently, Sandström *et al.*[12] showed that the anisotropic CC couplings (D_{CC} couplings) in liquid crystal molecules can be obtained by two-dimensional double quantum NMR experiments with carbon-13 at natural abundance. This is a big advantage and thus may provide a useful method for studying orientation and conformation of liquid crystal molecules in *mesophases*. The utilization of the CC couplings, however, becomes feasible only when the contribution of ΔJ_{CC} to the experimental D_{CC} is known or can safely be neglected. Therefore, in order to gain insight into the anisotropy of carbon−carbon coupling tensors in aromatic ring systems, it seems natural to study them, *i.e.*, $\Delta^n J_{CC}$ ($n = 1$, 2, and 3), in benzene. An earlier study of benzene[13] delt with the ratios of the D_{CC} values corrected for harmonic vibrations and showed that the couplings may indeed include a contribution from the spin−spin coupling anisotropy, but no estimate for the magnitude of the anisotropies could be given.

There are a few studies on semiempirical calculations of the CC spin−spin coupling tensors of benzene in the literature.[14,15] The only first principles study[6a] reports DFT results for the isotropic constants, but has neglected the SD contribution, however. As none of the previous theoretical works reports all the parameters of present interest, ${}^nJ_{CC}$ and $\Delta^n J_{CC}$, and since it is difficult to assess the validity of semiempirical work without reference to experimental results, the case calls for a systematic *ab initio* study, where all the different contributions to ${}^n\mathbf{J}_{CC}$ are calculated with varying basis sets and treatment of correlation.

In this study, we have derived the indirect carbon−carbon coupling constants ${}^nJ_{CC}$ for benzene by (a) utilizing the $^2H/^1H$ isotope effect on carbon shieldings in monodeuterated benzene (C_6H_5D) and recording the $^{13}C\{^1H\}$ spectrum and (b) recording the ^1H-coupled ^{13}C NMR spectrum of $^{13}C_6H_6$ and performing its complete analysis. The anisotropies of the coupling tensors, $\Delta^n J = {}^nJ_{||} - {}^nJ_{\perp}$, where the subscripts refer to the **J** tensor elements in the parallel and perpendicular directions, respectively, *with respect to the C_6 symmetry axis of benzene*, were determined by applying LC NMR. In the course of this work it turned out that even the natural abundance double-quantum ^{13}C NMR spectra of benzene dissolved in liquid crystals are observable in a reasonable time, and thus the D_{CC} couplings are available through this way as well. However, due to broad lines (proton decoupling causes temperature fluctuations and gradients which affect solute molecular orientation and the magnitude of D couplings as well as chemical shifts), their uncertainty is relatively high, making the method unsuitable for the detection of small anisotropic contributions in experimental D couplings, and consequently for the determination of spin−spin coupling anisotropies. Therefore, we decided to use fully carbon-13-enriched benzene, although its ^1H and ^{13}C NMR spectra (arising from 12 spin-1/2 nuclei) in liquid crystal solutions are extremely complex, also for the study of the CH and CC couplings. Besides, this method has a large benefit; all the D couplings can be determined from the *same spectra*, ensuring exactly the same experimental conditions. $^{13}C_6$-enriched benzene was dissolved in three thermotropic liquid crystals, and both the ^1H and ^{13}C NMR spectra were recorded. *Ab initio* calculations were performed for the tensors ${}^1\mathbf{J}_{CC}$, ${}^2\mathbf{J}_{CC}$, and ${}^3\mathbf{J}_{CC}$ using the MCSCF linear response method[4] with a single-reference wave function and also with multireference ones. In the latter the delocalized π-electron system was chosen as the multireference basis.

Experimental Section

NMR Spectroscopy. The spin−spin coupling constants were determined from neat benzene-d_1 (98% D; Cambridge Isotope Laboratories) by recording the $^{13}C\{^1H\}$ NMR spectrum with ^{13}C satellites on a Bruker DPX400 spectrometer, the operating frequencies being 100.61 and 400.13 MHz for ^{13}C and ^1H, respectively. In order to reach a sufficient signal-to-noise ratio, 2048 FIDs with 4k points were accumulated. A relaxation delay of 10 s and frequency range of 360 Hz were applied. The line width at half-height was ca. 0.3 Hz. The frequency of each resonance line was determined with the aid of the FITPLA program written in our research group.[16] These frequencies were fed to the iterative LEQUOR spectral analysis program[17] for the determination of coupling constants and chemical shifts, *i.e.*, isotope effects on ^{13}C shifts.

For the determination of the anisotropy of the CC spin−spin coupling tensors, ^{13}C-enriched benzene ($^{13}C_6H_6$ with 99% ^{13}C; Isotec Inc.) was dissolved in three thermotropic liquid crystals: (A) Merck ZLI 1167 (a mixture of three *p*(*n*-alkyl)*trans*,*trans*-bicyclohexyl-*p*′-carbonitriles), (B) Merck Phase 4 (eutectic mixture of *p*-methoxy-*p*′-(*n*-butyl)-azoxydibenzenes), and (C) the 58 wt %:42 wt % mixture of ZLI 1167 and Phase 4 (referred to as MIXTURE from here on), respectively. The liquid crystals ZLI 1167 and Phase 4 were chosen because they possess divergent properties. The anisotropy of the diamagnetic susceptibility, $\Delta\chi_m$, of the former is negative, and therefore its director orients perpendicularly to the external magnetic field. Phase 4, on the contrary, has a positive $\Delta\chi_m$, leading to the orientation of the director along the external field. Moreover, studies of solute molecules in these two liquid crystals have yielded geometric distortions of opposite signs. MIXTURE also has a positive $\Delta\chi_m$, but the positive and negative geometry distortions almost cancel each other.[18] There are bases to expect that other NMR properties of a solute, shielding and spin−spin coupling, also are least distorted in this particular liquid crystal mixture.[19] Samples A, B, and C contained 6.7, 10.3, and 8.4 mol % benzene, respectively, and they were introduced into 5-mm (o.d.) NMR tubes and degassed in a vacuum line. The ^1H and ^{13}C NMR spectra of each sample were recorded at 300 K (at this temperature the liquid crystals appear in the nematic phase) on a Bruker DPX400 spectrometer.

(11) (a) Vahtras, O.; Ågren, H.; Jørgensen, P.; Helgaker, T.; Jensen, H. J. Aa. *Chem. Phys. Lett.* **1993**, *209*, 201−6. (b) Perera, S. A.; Sekino, H.; Bartlett, R. J. *J. Chem. Phys.* **1994**, *101*, 2186−2191.

(12) Sandström, D.; Summanen, K. T.; Levitt, M. H. *J. Am. Chem. Soc.* **1994**, *116*, 9357−8.

(13) Diehl, P.; Bösiger, H.; Jokisaari, J. *Org. Magn. Reson.* **1979**, *12*, 282−283.

(14) (a) Blizzard, A. C.; Santry, D. P. *J. Chem. Phys.* **1971**, *55*, 950−63; **1973**, *58*, 4714. (b) Lazzeretti, P.; Taddei, F.; Zanasi, R. *J. Am. Chem. Soc.* **1976**, *98*, 7989−93. (c) Wray, V.; Ernst, L.; Lund, T.; Jakobsen, H. J. *J. Magn. Reson.* **1980**, *40*, 55−68.

(15) Pyykkö, P.; Wiesenfeld, L. *Mol. Phys.* **1981**, *43*, 557−80.

(16) van den Boogaart, A.; Ala-Korpela, M.; Jokisaari, J.; Griffiths, J. R. *Magn. Reson. Med.* **1994**, *31*, 347−58. Ala-Korpela, M.; Korhonen, A.; Keisala, J.; Hörkkö, S.; Korpi, P.; Ingman, L. P.; Jokisaari, J.; Savolainen, M. J.; Kesäniemi, Y. A. *J. Lipid Res.* **1994**, *35*, 2292−304.

(17) Diehl, P.; Kellerhals, H.; Niederberger, W. *J. Magn. Reson.* **1971**, *4*, 352−7.

(18) Jokisaari, J.; Hiltunen, Y. *Mol. Phys.* **1983**, *50*, 1013−23.

(19) Jokisaari, J.; Hiltunen, Y.; Lounila, J. *J. Chem. Phys.* **1986**, *85*, 3198−202.

The spectra were analyzed on PERCH software[20] using the peak-top-fit mode. The same samples, heated to the isotropic state (samples A and B, 350 K; sample C, 345 K), were also used for the determination of the carbon−proton and carbon−carbon spin−spin coupling constants. The particular goal was to find out their solvent dependence. The HH spin−spin coupling constants, J_{HH}, were adopted from ref 21 for benzene in ZLI 1167 and Phase 4, while for MIXTURE, the concentration-weighted average values were used. In each case, J_{HH} values were kept fixed in the iterative spectral analyses.

The typical run parameters for the samples in ^{13}C NMR spectra were the following: acquisition time 1.6 s, relaxation delay 1 ms, pulse angle 30°, and number of scans 128. The corresponding parameters in the ^1H runs of the oriented samples were 1.1 s, 5 s (here we used the inversion−recovery method to cancel the complicated baseline originating from liquid crystals), and 256 scans.

***Ab Initio* Calculations.** MCSCF linear response calculations of the spin−spin coupling tensors were carried out as described by Vahtras *et al.*[4] using the DALTON software.[22] Spin−spin coupling $\mathbf{J}_{ij}$ is a second-order molecular property; the corresponding energy term is bilinear in the magnetic moments of the nuclei i and j. DALTON employs a combination of expectation values (for the DSO contribution) and the MCSCF linear response formalism[23] (other terms), and the approach has been applied in several works reporting spin−spin coupling constants.[24] For details of the theory and implementation, we refer to the original paper.[4] We used the CCSD/cc-VTZ optimized equilibrium geometry of benzene reported by Brenner *et al.*,[25] where $r_{CC} = 1.393$ Å and $r_{CH} = 1.082$ Å. In one test calculation we also employed the geometry used in the experimental analysis of the data, $r_{CC} = 1.397$ Å and $r_{CH} = 1.085$ Å, to gain insight into the sensitivity of the results to geometry.

Correlated *ab initio* calculations, and those of the spin−spin coupling in particular, require the use of good atomic orbital basis sets. For molecules the size of benzene this becomes a serious bottleneck, as one often cannot reach the basis set limit in the calculated properties. In this work, we utilized two different basis sets, firstly, the TZP level set adopted originally from Huzinaga.[26] The set, denoted by HII, has been previously applied in nuclear shielding calculations.[27] In the context of spin−spin couplings it has been pointed out as not being fully saturated for small organic molecules.[24b] Nevertheless, it provides a reasonable basis (168 functions) to be used in large MCSCF expansions, which would currently be beyond our computational resources with more extended one-particle basis sets for benzene. Secondly, we took the TZ basis set of Schäfer *et al*.[28] augmented with two polarization functions[29] on each atom; p-type (exponents 1.407 and 0.388) for hydrogen and d-type (1.097 and 0.318) for carbon. The need to have extremely tight s-type basis functions on the nuclei for which the **J** tensor is calculated has been pointed out.[4,30] Consequently, we added three s-primitives to each carbon with the exponents 125 000, 900 000, and 6 000 000.[30b] At the same time, we also decontracted the carbon valence s- and p-shells and the hydrogen s-shell slightly, resulting in 252 contracted functions and the basis denoted here as TZ+s. As DALTON is presently limited to 255 molecular orbitals in MCSCF calculations, a larger basis set than TZ+s is unavailable for benzene. Considering previous experience,[7,24] the present TZ+s basis should be close to saturation even for the FC contribution. The contraction patterns of these basis sets are shown in Table 1.

Table 1. Basis Sets Used in the MCSCF Calculations[a]

basis		Gaussian functions: GTO	Gaussian functions: CGTO	contraction pattern[b]
HII	H	(5s1p)	[3s1p]	{311/1*}
	C	(9s5p1d)	[5s4p1d]	{51 111/2 111/1*}
TZ+s	H	(5s2p)	[4s2p]	{2 111/1*1*}
	C	(13s6p2d)	[10s4p2d]	{1 114 111 111/3 111/1*1*}

[a] Identifiers, numbers of primitive and contracted functions, and the corresponding contraction patterns are shown. Spherical Gaussians are used throughout. [b] Polarization functions are denoted by an asterisk.

In MCSCF calculations[31] the electronic wave function consists of a linear combination of several Slater determinants constructed by moving electrons out from the doubly occupied (in the SCF picture) molecular orbitals to the unoccupied (virtual) ones within the chosen active orbital space. Both the coefficients of the determinants and the orbitals are variationally optimized. For MCSCF to be successful, the active space must be chosen in a balanced way[27b] to contain the orbitals that are expected to participate most in electron correlation effects. The complete active space (CAS) wave function consists of all determinants that can be constructed within the active space, corresponding to full configuration interaction calculation in that limited space. The size of a CAS expansion rapidly becomes prohibitive as more electrons and orbitals are included in the active space, and the need to constrain the electron occupation numbers (and, consequently, limit the number of determinants in the wave function) in different parts of the active space arises. Then one has the restricted active space (RAS) method, in which the most common way to partition the active space is to use three subblocks of orbitals. The maximum number of holes can be specified in RAS1, which contains orbitals that are doubly occupied in the SCF wave function. RAS2 corresponds to the active space in CAS calculations: no constraints to the orbital occupation numbers are put there. In RAS3 one can specify the maximum number of particles (electrons), n_p. If RAS2 only contains orbitals that are doubly occupied in SCF, one has a single-reference wave function subjected to single, double, etc. (depending on n_p) excitations. This allows estimating dynamical correlation effects. Inclusion of one or more virtual orbitals into RAS2 gives the wave function a multireference character suitable for investigating static correlation.

We performed the present MCSCF calculations for benzene in the largest Abelian point group symmetry, D_{2h}, corresponding to the full D_{6h} point group of the molecule. The different active spaces used were chosen with the help of natural orbital occupation numbers calculated as eigenvalues of the MP2 spin-reduced one-particle density matrix, and are given in Table 2.

The molecular orbitals that comprise the delocalized π-electron system in benzene are best discussed with Hückel orbitals.[32] The HOMO−LUMO (highest occupied−lowest unoccupied molecular orbital) gap separates two doubly degenerate sets of orbitals arising from the carbon $p_\parallel$ atomic orbitals. These four orbitals are contained in our CAS-I calculations. CAS-II contains, additionally, the two nondegenerate delocalized π-orbitals positioned symmetrically below and above (in the energy scale) HOMO and LUMO, respectively. Both CAS-I and CAS-II are small multireference wave functions. RAS-I

(20) Laatikainen, R.; Niemitz, M.; Weber, U.; Sundelin, J.; Hassinen, T.; Vepsäläinen, J. *J. Magn. Reson.* A **1996**, *120*, 1−10.
(21) Diehl, P.; Bösiger, H.; Zimmermann, H. *J. Magn. Reson.* **1979**, *33*, 113−26.
(22) Helgaker, T.; Jensen, H. J. Aa.; Jørgensen, P.; Koch, H.; Olsen, J.; Ågren, H.; Bak, K. L.; Bakken, V.; Christiansen, O.; Halkier, A.; Dahle, P.; Heiberg, H.; Hettema, H.; Jonsson, D.; Kobayashi, R.; de Meras, A. S.; Mikkelsen, K. V.; Normann, P.; Ruud, K.; Taylor, P. R.; Vahtras, O. *DALTON, an electronic structure program;* 1996.
(23) Jørgensen, P.; Jensen, H. J. Aa.; Olsen, J. *J. Chem. Phys.* **1988**, *89*, 3654−61. Olsen, J.; Yeager, D. L.; Jørgensen, P. *Ibid.* **1989**, *91*, 381−8.
(24) (a) Barszczewicz, A.; Jaszunski, M.; Kamienska-Trela, K.; Helgaker, T.; Jørgensen, P.; Vahtras, O. *Theor. Chim. Acta* **1993**, *87*, 19−28. (b) Barszczewicz, A.; Helgaker, T.; Jaszunski, M.; Jørgensen, P.; Ruud, K. *J. Chem. Phys.* **1994**, *101*, 6822−8. (c) Ruud, K.; Helgaker, T.; Jørgensen, P.; Bak, K. L. *Chem. Phys. Lett.* **1994**, *226*, 1−10. (d) Barszczewicz, A.; Helgaker, T.; Jaszunski, M.; Jørgensen, P.; Ruud, K. *J. Magn. Reson. A* **1995**, *114*, 212−8.
(25) Brenner, L. J.; Senekowitsch, J.; Wyatt, R. E. *Chem. Phys. Lett.* **1993**, *215*, 63−71.
(26) Huzinaga, S. *Approximate Atomic Functions*; University of Alberta: Edmonton, 1971.
(27) (a) Schindler, M.; Kutzelnigg, W. *J. Chem. Phys.* **1982**, *76*, 1919−33. (b) Ruud, K.; Helgaker, T.; Kobayashi, R.; Jørgensen, P.; Bak, K. L.; Jensen, H. J. Aa. *Ibid.* **1994**, *100*, 8178−85.
(28) Schäfer, A.; Horn, H.; Ahlrichs, R. *J. Chem. Phys.* **1992**, *97*, 2571−7.
(29) Dunning, Jr., T. H. *J. Chem. Phys.* **1989**, *90*, 1007−23
(30) (a) Oddershede, J.; Geertsen, J.; Scuseria, G. E. *J. Phys. Chem.* **1988**, *92*, 3056−9. (b) Geertsen, J.; Oddershede, J.; Raynes, W. T.; Scuseria, G. E. *J. Magn. Reson.* **1991**, *93*, 458−71.
(31) Roos, B. O. In *Lecture Notes in Quantum Chemistry*; Roos, B. O., Ed.; Springer-Verlag: Berlin, 1992; pp 177−254.
(32) Atkins, P. W. *Molecular Quantum Mechanics*, 2nd ed.; Oxford University Press: Oxford, 1983; p 275.

Table 2. Active Molecular Orbital Spaces Used in the MCSCF Calculations[a]

wf	inactive[b]	RAS1	RAS2	RAS3	n_h	n_p	n_{SD}
CAS-I	64105300		00110011				12
CAS-II	64005300		00210021				104
RAS-0	21002100		43113210	53214321		2	19 194
RAS-I	42003200	22102100	00110011	32002210	2	2	94 210
RAS-II	42003200	22002100	00210021	32002200	2	2	982 274

[a] The numbers in each category denote the number of orbitals in the following eight symmetry species of the D_{2h} point group: A_g, B_{3u}, B_{2u}, B_{1g}, B_{1u}, B_{2g}, B_{3g}, and A_u. The maximum number of holes in RAS1, n_h, maximum number of particles in RAS3, n_p, and number of Slater determinants in the wave function, n_{SD}, are indicated. [b] A SCF calculation of benzene would be designated as (6411 5310/−/−/−) in the notation (inactive/RAS1/RAS2/RAS3).

and RAS-II allow single and double excitations out of the multireference basis furnished by CAS-I and CAS-II, respectively. RAS-0, on the other hand, is a single-reference wave function in which we allow up to double excitations from all the occupied valence orbitals into a fairly large virtual active space. The present active spaces comprise 21%, 26%, 73%, and 55% of the total MP2 occupation in the virtual orbitals in CAS-I, CAS-II, RAS-0, and RAS-I/RAS-II, respectively. In the occupied (in the SCF sense) orbitals the corresponding (hole) percentages are 28, 37, 99 and 81. As the RAS-I and RAS-II wave functions consist of almost 100 000 and 1 000 000 Slater determinants (in the respective order), we have chosen to calculate only the most demanding contributions, FC, and SD/FC (moreover SD for RAS-I), to $^nJ_{CC}$ using them. All the contributions (DSO, PSO, SD, FC and SD/FC) are calculated for CAS-I and CAS-II wave functions, and all but DSO for RAS-0.

Results and Discussion

A. Experimental Spin−Spin Coupling Constants. The indirect HH and CC spin−spin couplings, $^nJ_{HH}$ and $^nJ_{CC}$, of normal, protonated benzene are not directly measurable in isotropic solutions due to the chemical equivalence of the protons and carbon-13 nuclei, respectively. There exist, however, various means to overcome this problem. For example, the necessary nonequivalence between the carbon-13 nuclei can be introduced without significantly affecting the couplings by substituting deuterium for a hydrogen atom (for a discussion of isotope effects on spin−spin couplings, see ref 33). This substitution leads to a change of the molecular vibrational states and, therefore, to a shielding difference between the nuclei. This technique was applied in the present study; the CC spin−spin coupling constants were derived from the ^{1}H-decoupled ^{13}C satellite spectra in the ^{13}C NMR spectra of C_6H_5D with ^{13}C at natural abundance. The results, shown in Table 3, are in excellent agreement with those reported by Roznyatovsky *et al.*[34]

From the accuracy point of view, it is of vital importance to measure the *J* couplings in conditions corresponding as closely as possible to the ones used for obtaining the *D* couplings. In the present study, we used $^{13}C_6H_6$ dissolved in the three liquid crystal samples heated to the isotropic state and recorded the proton-coupled ^{13}C NMR spectra. The CH and CC couplings resulting from the spectral analyses are given in Table 3, too. It is seen that the J_{CH} and J_{CC} couplings are not very sensitive to medium effects. However, one has to remember that even a small change in *J* is reflected in the corresponding *D* coupling, and this may lead to a marked apparent change in the anisotropy of the coupling tensor.

Table 3. Experimental and Calculated CH and CC Spin−Spin Coupling Constants in Benzene[a]

	experimental				
coupling	C_6H_5D[b]	ZLI 1167[c]	MIXTURE[d]	Phase 4[e]	calculated
$^1J_{CH}$		158.550(6)	158.310(9)	158.41(1)	176.7[f]
$^2J_{CH}$		1.032(8)	1.04(1)	1.09(1)	−7.4[f]
$^3J_{CH}$		7.517(5)	7.62(2)	7.72(1)	11.7[f]
$^4J_{CH}$		−1.28(1)	−1.23(2)	−1.44(1)	−4.6[f]
$^1J_{CC}$	55.87(2)	55.98(1)	55.811(4)	55.83(2)	70.9[g]
$^2J_{CC}$	−2.486(24)	−2.49(1)	−2.519(9)	−2.434(7)	−5.0[g]
$^3J_{CC}$	10.111(25)	10.099(9)	10.090(6)	10.12(2)	19.1[g]

[a] Values in hertz. The figure in parentheses after the experimental values is the standard deviation in units of the last digit. [b] Neat monodeuteriobenzene. The coupling constants were derived from the ^{1}H-decoupled ^{13}C NMR spectrum. [c] $^{13}C_6H_6$ dissolved in the liquid crystal ZLI 1167. The sample was heated to the isotropic state (T = 350 K). The coupling constants were derived from the ^{1}H-coupled ^{13}C NMR spectrum. [d] As in footnote *c*, but the solvent was liquid crystal MIXTURE (see the text) and the sample was heated to the isotropic state at T = 345 K. [e] As in footnote *c*, but the solvent was liquid crystal Phase 4. [f] CAS-II/TZ+s calculation. [g] RAS-II/HII calculation.

The analysis of a second-order spectrum yields the relative signs of the spin−spin coupling constants. It is generally accepted that the one-bond CH couplings are positive. In our analysis the *ortho*, *meta*, and *para* CC couplings appear to be positive, negative, and positive, respectively. This is the very first time that this sign combination has been confirmed experimentally. Earlier the signs were concluded from the corresponding ones in substituted benzenes.[35]

B. *Ab Initio* Spin−Spin Coupling Constants. The results of the MCSCF calculations for $^nJ_{CC}$ and $^nJ_{CH}$ are given in Table 4. The best of these are also compared to experimental ones in Table 3.

The results show a monotonic decrease in the absolute values of the CC coupling constants with the size of the wave function expansion. This is in line with the earlier findings indicating that MCSCF wave functions tend to underestimate correlation effects in *J*.[24] The signs of $^nJ_{CC}$, however, are found to be unchanged; even the modest CAS-I calculation is able to reproduce the experimental sign combination. This is in contrast to results at the SCF level (not shown), where only $^1J_{CC}$ is of correct sign. The results of a small multireference expansion, CAS-II, and a relatively elaborate single-reference calculation, RAS-0, are comparable, except for the *ortho* coupling where the latter ends up closer to the experimental value. It may be noted here that Brenner *et al.*[25] did not find significant multireference character in their study of the structure and in-plane force field of benzene. However, further improvement in $^nJ_{CC}$ can be seen in the two multireference RAS calculations, particularly in the *meta* coupling.

Compared with the experimental results, even the best of the present calculations gives too large (in magnitude) $^nJ_{CC}$ couplings, but the trend in increasing the number of correlating orbitals would apparently lead to a fairly good agreement, if continued further. Presently, the agreement is best in the *ortho* coupling while the differences in $^2J_{CC}$ and $^3J_{CC}$ are still large. The signs, as already stated, are consistently correct. This is not the case for CAS $^nJ_{CH}$, however, where the $n = 2$ coupling is calculated to have a negative sign contrary to experiment. There is no doubt in the correctness of the experimental result, as the positive sign is also obtained theoretically in ref 6a. The two-bond CC and CH couplings appear to be more difficult than the corresponding one- and three-bond couplings.[8] In the present work the magnitude of the calculated $^nJ_{CH}$ couplings is also overestimated.

(33) Sergeyev, N. M. In *NMR Basic Principles and Progress*; Diehl, P., Fluck, E., Günther, H., Kosfeld, R., Seelig, J., Eds.; Springer-Verlag: Berlin, 1990; Vol. 22; pp 31−80.

(34) Roznyatovsky, V. A.; Sergeyev, N. M.; Chertkov, V. A. *Magn. Reson. Chem.* **1991**, *29*, 304−7.

(35) Krivdin, L. B.; Della, E. W. *Prog. Nucl. Magn. Reson. Spectrosc.* **1991**, *23*, 301−610.

Table 4. Results of the MCSCF Calculations for the CH and CC Spin−Spin Coupling Constants in Benzene[a]

basis	wf	230 + E	$^1J_{CH}$	$^2J_{CH}$	$^3J_{CH}$	$^4J_{CH}$	$^1J_{CC}$	$^2J_{CC}$	$^3J_{CC}$
HII	CAS-I	−0.793 885	191.8	−15.6	18.3	−11.4	107.8	−28.1	32.1
TZ+s	CAS-I	−0.819 770	182.5	−12.4	16.3	−9.3	104.8	−26.8	31.1
TZ+s	CAS-I[b]	−0.819 033	184.7	−12.9	16.9	−9.9	106.7	−28.4	32.5
HII	CAS-II	−0.826 472	185.1	−9.8	12.9	−6.1	95.2	−15.3	19.6
TZ+s	CAS-II	−0.851 546	176.7	−7.4	11.7	−4.6	93.1	−14.9	19.4
HII	RAS-0[c]	−1.151 394					77.8	−12.2	19.4
HII	RAS-I[d]	−1.003 442					72.4	−5.9	19.4
HII	RAS-II[e]	−1.011 383					70.9	−5.0	19.1
	DFT[f]		150.7	2.6	7.1	−0.9	53.1	−0.4	8.8
	REX[g]		74.0				35.3		
	INDO[h]						72.8	−11.5	13.4
	INDO[i]						53.9	−10.6	14.3
	INDO[j]						54.7		

[a] Values in hertz calculated at the CCSD/cc-VTZ geometry:[25] r_{CC} = 1.393 Å and r_{CH} = 1.082 Å. The basis sets and the type of wave function (see Tables 1 and 2, respectively) are indicated for each calculation, together with the calculated total energy (Ha). Also some theoretical values from the literature are listed for comparison. [b] Calculated at the geometry used in the analysis of the experimental data. [c] DSO contribution calculated at the CAS-II/HII level. [d] DSO and PSO contributions calculated at the CAS-II/HII level. [e] DSO and PSO contributions calculated at the CAS-II/HII level and SD contribution at the RAS-I/HII level. [f] Reference 6a; finite perturbation DFT with no spin-dipole contribution calculated. [g] Reference 15; relativistically parametrized extended Hückel calculation. [h] Reference 14c; INDO (intermediate neglect of differential overlap)−finite perturbation calculation with PSO, SD and FC contributions. [i] Reference 14b; INDO-coupled Hartree−Fock calculation with PSO, SD, and FC contributions. [j] Reference 14a; INDO−self-consistent perturbation calculation with PSO, SD, and FC contributions.

Table 5. Contributions of the Different Physical Mechanisms to the Calculated CC Spin−Spin Couplings in Benzene[a]

coupling	wf	DSO	PSO	SD	FC	total
$^1J_{CC}$	CAS-I	0.4	−6.6	3.6	110.5	107.8
	CAS-II	0.4	−6.1	1.9	99.1	95.2
	RAS-0[b]		−6.6	3.0	81.0	77.4
	RAS-I[c]			1.5	76.6	72.4
	RAS-II[d]				75.1	70.9
	INDO[e]		−12.3	3.0	63.1	53.9
	INDO[f]		−12.8	3.2	64.3	54.7
$^2J_{CC}$	CAS-I	−0.2	0.0	−3.1	−24.8	−28.1
	CAS-II	−0.2	0.0	−1.4	−13.7	−15.3
	RAS-0[b]		0.0	−2.6	−9.4	−12.1
	RAS-I[c]			−1.1	−4.7	−5.9
	RAS-II[d]				−3.7	−5.0
	INDO[e]		0.9	−2.5	−9.0	−10.6
$^3J_{CC}$	CAS-I	0.1	0.4	3.8	27.8	32.1
	CAS-II	0.1	0.3	2.1	17.0	19.6
	RAS-0[b]		0.4	3.4	15.4	19.3
	RAS-I[c]			1.8	17.1	19.4
	RAS-II[d]				16.8	19.1
	INDO[e]		1.0	3.8	9.6	14.3

[a] Values in hertz calculated with the HII basis set at the CCSD/cc-VTZ geometry.[25] [b] DSO contribution to the indicated total couplings taken from the CAS-II/HII calculation. [c] DSO and PSO contributions to the total couplings taken from the CAS-II/HII calculation. [d] DSO and PSO contributions to the total couplings taken from the CAS-II/HII calculation; SD contribution from RAS-I/HII. [e] See footnote *i* in Table 4. [f] See footnote *j* in Table 4.

The contributions of the different physical mechanisms to the calculated CC coupling constants are shown in Table 5. Here, our findings parallel those of the early semiempirical work by Lazzeretti *et al.*[14b] The FC contribution is found to be the dominating one in all $^nJ_{CC}$ couplings and calculations. Both DSO and PSO give very small contributions to the *meta* and *para* couplings. However, omission of the PSO term would lead to a significant overestimation of $^1J_{CC}$. It is notable that the pattern formed by the different contributions to the *ortho* CC coupling in benzene closely matches that for $^1J_{CC}$ in several other hydrocarbons, suggesting that this may be a general characteristic of one-bond CC couplings between sp^2-hybridized carbons.[8b,24ac,36] The SD contribution was neglected in DFT work by Malkin *et al.*[6a] We find that, while less important than PSO in $^1J_{CC}$, SD is clearly more significant than PSO for the other two CC couplings. We agree with ref 6a in that the neglect of the SD term is easily masked by errors in the dominating—notorious—FC contribution in calculations of the present level of accuracy. However, the spin−dipolar interaction has a significant contribution in the CC coupling anisotropies (see below), particularly through the SD/FC cross-term.[37]

Improvement in the correlation treatment, considered here to be parallel to the length of the determinantal expansion, is expectedly confined mainly to the systematic decrease in the magnitude of the FC contribution.[38] Certainly one is allowed to use a lower level of theory (even SCF in the present case) for the DSO and PSO contributions than for FC.[39] The SD contribution is also affected by correlation, but its small magnitude allows one to use low-level results in interpreting the general trends here as well. It was noted in ref 40 that even a small multireference expansion is sufficient to remedy the triplet instability problem, as evidenced by our CAS-I and CAS-II calculations, too. From the relative success of the present RAS-0 single-reference calculation, it is clear that the FC terms in both $^nJ_{CC}$ and $^nJ_{CH}$ contain a large fraction of dynamical electron correlation, which is absent in our two CAS wave functions. Indeed, the large RAS-I and RAS-II calculations indicate that the FC contribution is still not fully converged with respect to correlation treatment in the best of our calculations. The next step would be to use the large all-valence active space of the RAS-0 wave function with the multireference bases of CAS-I or CAS-II. This is unfortunately beyond our current resources, however. The main progress in such a calculation is to be expected in $^3J_{CC}$, where our present calculations seem to converge at too high a value.

Regarding the one-electron basis sets used, HII is not saturated as can be seen from the difference in the CAS-I and CAS-II calculations, which have also been performed with the better polarized TZ+s set with tight s-functions. The $^nJ_{CH}$ couplings are sensitive to the basis set quality as changes ranging from 5% to 25% (to the direction of the experimental results) are seen when the basis is improved. The $^nJ_{CC}$ values are less sensitive: the corresponding improvement is 5% or below at

(36) Scuseria, G. E. *Chem. Phys. Lett.* **1986**, *127*, 236−41.

(37) (a) Buckingham, A. D.; Love, I. *J. Magn. Reson.* **1970**, *2*, 338−51. (b) Lazzeretti, P.; Zanasi, R. *J. Chem. Phys.* **1982**, *77*, 2448−53.

(38) Scuseria, G. E.; Geertsen, J.; Oddershede, J. *J. Chem. Phys.* **1989**, *90*, 2338−43.

(39) Overill, R. E.; Saunders, V. R. *Chem. Phys. Lett.* **1984**, *106*, 197−200. Scuseria, G. E. *Chem. Phys.* **1986**, *107*, 417−27.

(40) Laaksonen, A.; Kowalewski, J.; Saunders, V. R. *Chem. Phys.* **1983**, *80*, 221−7. Laaksonen, A. I.; Saunders, V. R. *Chem. Phys. Lett.* **1983**, *95*, 375−8.

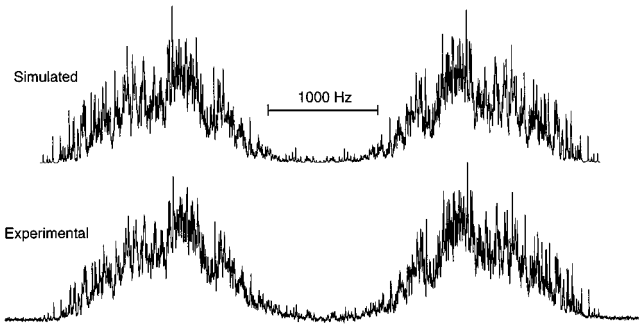

Figure 1. Simulated and experimental ^{13}C NMR spectrum of $^{13}C_6H_6$ in the nematic phase of the ZLI 1167 liquid crystal.

the CAS-I level and smaller (3% or below) at the CAS-II level. If we scale the results of our best calculation, RAS-II, by the fractional change seen in CAS-II results, we note that the major possibilities of improvement in $^nJ_{CC}$ upon the present level indeed lie in the correlation treatment, not in the atomic basis set used.

Comparison of the CAS-I/TZ+s calculations performed using different geometries for the molecule reveals changes on the order of 2 Hz in all calculated CC coupling constants, which, however, is insignificant regarding the present overall accuracy. The sensitivity of the CH couplings to geometry appears to be negligible, though the change is of the expected direction for one-bond couplings,[41] *i.e.*, increased coupling for increased bond length. The FC contribution is almost solely responsible for the observed difference.

The results on the application of the semiempirical INDO (intermediate neglect of differential overlap) method in the literature[14] are comparable to our best *ab initio* ones. Lazzeretti *et al.*[14b] and Wray *et al.*[14c] calculated all the $^nJ_{CC}$ couplings. References 14a,b reported values for the *ortho* coupling essentially in exact agreement with the experimental results. However, the approaches followed in these computations involved a fit of the spin density and the expectation value $\langle r^{-3}\rangle$ at the nuclei to reproduce the experimental couplings of several compounds including benzene. While INDO results for $^3J_{CC}$ are somewhat superior to ours, $^2J_{CC}$ is off by an order of magnitude in INDO. Overall, the semiempirical methods do a respectable job in the calculation of the spin−spin coupling constants in benzene. However, as they are known to sometimes fail dramatically, they need to be used with care.[6a,37b]

The agreement of the sole first principles calculation (until now) by Malkin and co-workers[6a] with experiment is impressive. Their remaining error is more or less due to the neglected SD contribution to the CC couplings, which could be taken, *e.g.*, from our Table 5. Particularly, the difficult two-bond couplings are very well calculated. It is unclear if the present MCSCF linear response method would be superior to the approach of ref 6a if we were able to use a larger active space in a multireference MCSCF expansion. However, DFT remains certainly the more cost-effective method.

C. Experimental Anisotropy of the CC Spin−Spin Coupling Tensors. For the determination of the anisotropy of the carbon−carbon spin−spin coupling tensors, both the ^1H and ^{13}C NMR spectra were recorded at 300 K, where all three samples appear in the nematic phase. However, the final *D* couplings were analyzed from the spectrum of better quality: in ZLI 1167 and Phase 4 the ^{13}C spectrum was chosen, whereas in MIXTURE the ^1H spectrum was used. Figure 1 displays, to give an example, the experimental and simulated ^{13}C NMR spectrum of $^{13}C_6H_6$ in the ZLI 1167 liquid crystal. The analysis of such a spectrum yields altogether ten *D* couplings: three D_{HH} couplings, four D_{CH} couplings, and three D_{CC} couplings.

The NMR spin Hamiltonian appropriate for spin-1/2 nuclei in molecules partially oriented in uniaxial liquid crystal solvents can be written in the high-field approximation as[3]

$$\hat{H} = -B_0/(2\pi)\sum_i \gamma_i(1-\sigma_i)\hat{I}_{iz} + \sum_{i<j} J_{ij}\hat{\mathbf{I}}_i\cdot\hat{\mathbf{I}}_j + \sum_{i<j}(D_{ij} + (1/2)J_{ij}^{\text{aniso}})(3\hat{I}_{iz}\hat{I}_{jz} - \hat{\mathbf{I}}_i\hat{\mathbf{I}}_j) \quad (1)$$

where B_0 is the magnetic field of the spectrometer (in the *z* direction), γ_i, $\hat{\mathbf{I}}_i$, and σ_i are the gyromagnetic ratio, dimensionless spin operator, and nuclear shielding (sum of the isotropic and anisotropic contributions) of nucleus *i*, respectively. The direct dipolar coupling D_{ij} is defined as

$$D_{ij} = -\mu_0\hbar\gamma_i\gamma_j S_{ij}/(8\pi^2 r_{ij}^3) \quad (2)$$

where S_{ij} is the order parameter of the internuclear vector $\mathbf{r}_{ij}$ with respect to $\mathbf{B}_0$, and μ_0 and $\hbar$ have their usual meanings. The experimentally available couplings in a molecule dissolved into a liquid crystal, D_{ij}^{exp}, can be expressed as a sum of several contributions:

$$D_{ij}^{\text{exp}} = D_{ij} + (1/2)J_{ij}^{\text{aniso}} = D_{ij}^{\text{eq}} + D_{ij}^{\text{ah}} + D_{ij}^{\text{h}} + D_{ij}^{\text{d}} + (1/2)J_{ij}^{\text{aniso}} \quad (3)$$

On the right-hand side of eq 3, D_{ij}^{eq} is the dipole−dipole coupling corresponding to the equilibrium structure of the molecule, D_{ij}^{ah} arises from the anharmonicity of the vibrational potential, D_{ij}^{h} is the contribution from the harmonic vibrations, and D_{ij}^{d}, the deformational contribution, is due to the correlation between vibrational and reorientational motions (the solvent dependence of molecular geometry stems from this term). The term J_{ij}^{aniso} can be, in the general case, presented in the form

$$J_{ij}^{\text{aniso}} = (2/3)(\sum_{\alpha\beta} S_{\alpha\beta}{}^D J_{ij\alpha\beta})P_2(\cos\theta) = (2/3)\Delta J_{ij} S^D P_2(\cos\theta) \quad (4)$$

where $S_{\alpha\beta}{}^D$ and $J_{ij\alpha\beta}$ are elements of the Saupe ordering tensor and the spin−spin coupling tensor, respectively, P_2 is the second-order Legendre polynomial, and θ is the angle between the external magnetic field and the liquid crystal director, **n**. The last equality in eq 4 is valid for a molecule with C_3 or higher symmetry. S^D is the order parameter of the molecular symmetry axis with respect to **n**.

In order to obtain a reliable value for J_{ij}^{aniso} and, consequently, for ΔJ_{ij}, one has to evaluate the vibrational and deformational contributions to D_{ij}^{exp} (see eq 3). The program MASTER[42] was used for this purpose. MASTER evaluates the harmonic vibrational corrections to the *D* couplings from available force fields, and the deformational corrections due to the anisotropic forces between the solute (benzene in the present case) and liquid crystal molecules. In the present study, the harmonic in-plane and out-of-plane force fields of benzene were adopted from the studies by Scherer.[43] Since the so-called r_α geometry of benzene is used in the MASTER calculations, the effect of the anharmonicity of the vibrational potential is automatically taken into account.[10] To gain insight into the importance of the various contributions, Table 6 lists the relevant values, D^{eq}, D^{h}, D^{d}, D^{calc}, and D^{exp}, for each interacting nuclear pair of

(41) Jameson, C. J.; Osten, H.-J. *J. Am. Chem. Soc.* **1986**, *108*, 2497−503.

(42) Wasser, R.; Kellerhals, M.; Diehl, P. *Magn. Reson. Chem.* **1989**, *27*, 335−9.

(43) Scherer, J. R. *Spectrochim. Acta* **1964**, *20*, 345−58; **1967**, *23A*, 1489−97.

Table 6. Calculated Dipole−Dipole Couplings, D^{calc}, with the Equilibrium, D^{eq}, Harmonic, D^{h}, and Deformational, D^{d}, Contributions to the Experimental Anisotropic Couplings for Benzene Dissolved in the MIXTURE Liquid Crystal Solvent[a]

coupling	D^{eq}	D^{h}	D^{d}	D^{calc}	D^{exp}
$^1D_{HH}$	−701.16	9.78	−1.99	−693.36	−693.368(7)
$^2D_{HH}$	−134.94	0.98	−0.27	−134.23	−134.220(9)
$^3D_{HH}$	−87.65	0.40	−0.14	−87.39	−87.417(12)
$^1D_{CH}$	−2108.96	158.55	−14.23	−1964.64	−1964.637(14)
$^2D_{CH}$	−269.33	5.08	−0.58	−264.83	−264.790(9)
$^3D_{CH}$	−68.43	0.48	−0.08	−68.03	−68.131(9)
$^4D_{CH}$	−46.20	0.18	−0.01	−46.02	−46.022(12)
$^1D_{CC}$	−248.79	1.83	−0.44	−247.40	−248.217(21)
$^2D_{CC}$	−47.88	0.03	0.05	−47.80	−47.569(20)
$^3D_{CC}$	−31.10	−0.05	0.08	−31.07	−31.613(32)
ΔA_{CH}	3.71(13)	η_{CC}			−0.33(3)
ΔA_{CC}	8.74(159)	$S^D = S^D P_2$			−0.17869
η_{CH}	1.45(30)	RMS error			0.0465 Hz

[a] All values are given in hertz. The anisotropic interaction parameters, ΔA_{CH}, ΔA_{CC} (10^{-22} J), η_{CH}, and η_{CC}, and the order parameters, S^D (with respect to the liquid crystal director) and $S^D P_2$ (with respect to the external magnetic field), are given at the bottom of the table. The figures in parentheses give the parameter error in units of the last digit quoted. See the text for details on the composition of MIXTURE.

benzene in the MIXTURE solvent (corresponding tables for ZLI 1167 and Phase 4 are available as supporting information).

Once the various contributions are known, the anisotropic contribution, J_{ij}^{aniso}, is obtained from

$$J_{ij}^{aniso} = 2[D_{ij}^{exp} - (D_{ij}^{eq} + D_{ij}^{h} + D_{ij}^{d})] = 2(D_{ij}^{exp} - D_{ij}^{calc}) \quad (5)$$

and, thus, the anisotropy from

$$\Delta J_{ij} = 3(D_{ij}^{exp} - D_{ij}^{calc})/[S^D P_2(\cos\theta)] \quad (6)$$

The indirect contributions to the D_{CC}^{exp} values, *i.e.*, $D_{ij}^{exp} - D_{ij}^{calc}$ in eq 6, for benzene in the three liquid crystals are results of separate MASTER calculations. In each case, the ratio of the CH (1.085 Å) and CC (1.397 Å) bond lengths, r_{CH}/r_{CC}, was fixed to 0.777. This is the value obtained on one hand by combining electron diffraction and infrared data[44] and on the other hand by combining the data obtained in the ZLI 1167 and Phase 4 liquid crystals.[2b] The calculation procedure follows the one applied by Lounila and Diehl[2b] except that the bond length ratio was fixed. The intermolecular interaction tensor (traceless and symmetric) is formed from contributions acting on the CH and CC bonds of the solute; thus, the interactions are completely determined by four interaction parameters: ΔA_{CH}, η_{CH}, ΔA_{CC}, and η_{CC}, ΔA denoting the anisotropy and η the asymmetry of a tensor. The values of these parameters were determined from seven experimental D couplings: three HH couplings and four CH couplings, weighted by their standard deviations. The order parameter S^D (referenced to the liquid crystal director) is obtained with the aid of the interaction parameters, and consequently, it is not an independent parameter. The results for MIXTURE are also shown in Table 6.

D. *Ab Initio* Anisotropies of Spin−Spin Coupling Tensors. The calculated results for the anisotropies of CH and CC spin−spin couplings are given and compared to experimental ones in Table 7. Exactly the same pattern as with the isotropic couplings $^nJ_{CC}$ is apparent also with the anisotropies Δ^nJ_{CC}: the sign combination in the *ortho*, *meta*, and *para* couplings equals

(44) Tamagawa, K.; Iijima, T.; Kimura, M. *J. Mol. Struct.* **1976**, *30*, 243−53.

Table 7. Experimentally and Theoretically Determined Anisotropies of the CH and CC Spin−Spin Couplings in Benzene[a]

basis	wf	Δ^1J_{CH}	Δ^2J_{CH}	Δ^3J_{CH}	Δ^4J_{CH}	Δ^1J_{CC}	Δ^2J_{CC}	Δ^3J_{CC}
HII	CAS-I	32.7	−12.4	7.2	−10.0	41.6	−41.5	40.8
TZ+s	CAS-I	32.2	−12.9	7.0	−10.4	40.5	−40.6	39.9
TZ+s	CAS-I[b]	32.6	−13.4	7.4	−10.8	42.9	−42.9	42.2
HII	CAS-II	27.8	−8.0	2.8	−5.9	19.1	−20.6	20.5
TZ+s	CAS-II	28.0	−9.2	3.3	−6.9	19.1	−20.8	20.9
HII	RAS-0[c]					25.6	−27.4	26.6
HII	RAS-I[d]					12.3	−13.9	14.0
HII	RAS-II[e]					11.0	−12.7	12.8
	REX[f]	43.8				29.1		
exp in ZLI 1167						21.2	−5.2	8.7
exp in MIXTURE						13.8	−3.9	9.1
exp in Phase 4						17.5	−2.5	10.7
exp average						17.5	−3.9	9.5

[a] Anisotropies in hertz with respect to the molecular C_6 axis of symmetry, $\Delta J = J_{||} - J_{\perp}$. [b] Calculated at the geometry used in the analysis of the experimental data. [c] DSO contribution calculated at the CAS-II/HII level. [d] DSO and PSO contributions calculated at the CAS-II/HII level. [e] DSO and PSO contributions calculated at the CAS-II/HII level and SD contribution at the RAS-I/HII level. [f] See footnote *g* in Table 4.

the experimental one in all calculations, and the magnitudes of the parameters decrease with the computational effort toward the experimental results. The agreement of the CAS-II calculation is, again, comparable with RAS-0, albeit the former now comes closer to the experimental values. It is difficult to say on the basis of these calculations if this may be interpreted to mean that the anisotropies are more affected by static correlation than the traces of $^n\mathbf{J}_{CC}$. The overall agreement with experiment is good in Δ^1J_{CC}, where the result is slightly below the experimental value for the MIXTURE solvent, which is supposed to be the least affected by anisotropic medium effects. Our final (RAS-II) *para* coupling anisotropy is less overestimated than the corresponding coupling constant. In Δ^2J_{CC} we are farther off than in $^2J_{CC}$; here the overshoot is a drastic one. In this kind of a comparison one must keep in mind that it is very difficult to give error estimates for the present experimental results. If the deviation of the experimental Δ^nJ_{CC} from one liquid crystal solvent to another is taken as an indication of the experimental uncertainty, our present *ab initio* calculations can be considered to perform satisfactorily.

It is notable that the calculated sign combinations of both Δ^nJ_{CC} and Δ^nJ_{CH} match exactly those of the calculated isotropic coupling constants. A SCF-level calculation (not shown) predicts the wrong sign for all Δ^nJ_{CC} values.

The experimental values for Δ^nJ_{CH} are not available for comparison. The magnitudes of the calculated Δ^nJ_{CH} are seen to decrease with increasing correlation, too. The utilization of the CH couplings in the analysis of the experimental results is well justified on the basis of the following facts. The best calculated *ab initio* anisotropies Δ^nJ_{CH} (CAS-II/TZ+s) overestimate the true values. Extrapolating on the basis of the trend apparent in Δ^nJ_{CC}, the $n \geq 2$ CH coupling anisotropies are seen to be very small (around 5 Hz or below), making the corresponding $(1/2)^nJ_{CH}^{aniso}$ (eq 3) also small. Despite the fact that the limiting value of Δ^1J_{CH} probably remains above 10 Hz, the corresponding $(1/2)^1J_{CH}^{aniso}$ is negligible compared to $^1D_{CH}^{exp}$. The uncertainties in $^1D_{CH}^{h}$ and $^1D_{CH}^{d}$, caused by the respective errors in the harmonic force field and the approximations of the deformational model, greatly exceed that of $(1/2)^1J_{CH}^{aniso}$.

We list in Table 8 the contributions of the different mechanisms to Δ^nJ_{CC}. As in refs 24d and 37b, the contribution of the SD/FC term is a very important one in all parameters and for both single-reference and multireference wave functions. The anisotropy of the *ortho* coupling has a large (in fact dominating)

Table 8. Contributions of the Different Physical Mechanisms to the Calculated Anisotropies of CC Spin−Spin Couplings in Benzene[a]

anisotropy	wf	DSO	PSO	SD	SD/FC	total	η
Δ^1J_{CC}	CAS-I	−2.3	10.3	4.6	29.0	41.6	0.363
	CAS-II	−2.3	9.5	2.0	9.9	19.1	0.444
	RAS-0[b]		10.3	3.8	13.8	25.6	0.484
	RAS-I[c]			1.5	3.5	12.3	0.555
	RAS-II[d]				2.3	11.0	0.570
Δ^2J_{CC}	CAS-I	−0.3	0.3	−4.4	−37.1	−41.5	0.011
	CAS-II	−0.3	0.3	−1.9	−18.7	−20.6	0.019
	RAS-0[b]		0.3	−3.8	−23.6	−27.4	0.008
	RAS-I[c]			−1.5	−12.4	−13.9	0.016
	RAS-II[d]				−11.3	−12.7	0.017
Δ^3J_{CC}	CAS-I	−0.5	−0.6	5.6	36.3	40.8	−0.063
	CAS-II	−0.5	−0.6	3.2	18.4	20.5	−0.096
	RAS-0[b]		−0.7	5.1	22.8	26.6	−0.105
	RAS-I[c]			2.7	12.3	14.0	−0.111
	RAS-II[d]				11.2	12.8	−0.111

[a] Anisotropies (Hz) are given with respect to the C_6 symmetry axis of the molecule, which is the third principal axis of the **J** tensors. Axis one is always the internuclear axis, and axis two is perpendicular to axes one and three. The last column contains the asymmetry parameter $\eta = (J_{11} - J_{22})/J_{33}$. [b] DSO contribution to the total anisotropies calculated at the CAS-II/HII level. [c] DSO and PSO contributions to the total anisotropies at the CAS-II/HII level. [d] DSO and PSO contributions to the total anisotropies at the CAS-II/HII level; SD contribution at the RAS-I/HII level.

contribution from the PSO mechanism, while both DSO and PSO can be neglected in Δ^2J_{CC} and Δ^3J_{CC}. The decrease in the SD/FC term with the length of the wave function expansion is a very dramatic one: the ratio of the results of the smallest and the largest of the present wave functions is over ten in Δ^1J_{CC} and about three in the two other CC coupling anisotropies. In the *ortho* coupling anisotropy even the SD contribution is comparable in magnitude with the limiting values of SD/FC. SD is a very time-consuming contribution to calculate, and unfortunately, it is significantly affected by electron correlation, as can be seen in Table 8. The DSO and PSO terms can be calculated very well at a lower level of theory in contrast to SD/FC.

Augmenting the atomic orbital basis affects Δ^nJ_{CC} very little: the changes are 2% or less at the CAS-II level and, contrary to $^nJ_{CC}$, to higher absolute values of the parameters. The sensitivity to the choice of geometry is similar to that in the trace of the tensors. The present HII basis set is found to be quite reasonable for the calculation of $^n\mathbf{J}_{CC}$ in benzene. As noted above, improvements upon the present calculations must be sought from a more efficient treatment of electron correlation.

Pyykkö and Wiesenfeld[15] reported the *ortho* CC coupling anisotropy for using the REX (relativistically parametrized extended Hückel) method. Their result is quite sensibly within the range of our present *ab initio* ones. The corresponding Δ^1J_{CH} appears also to be reasonable. Finally, we note that the **J** tensor elements, $J_{||} = J + 2\Delta J/3$ and $J_{\perp} = J - \Delta J/3$, from the present study can be easily obtained from the calculated and experimental couplings, J, and anisotropies, ΔJ.

Conclusions

We have established experimentally the sign combinations of $^nJ_{CC}$ and Δ^nJ_{CC} in the prototype aromatic hydrocarbon, benzene. The signs are positive, negative, and positive for the *ortho, meta*, and *para* couplings and coupling anisotropies. The magnitudes of the anisotropies have been determined with good reliability by performing the analysis of the NMR spectrum of the largest spin system oriented in a liquid crystal ever. The experimental sign combinations of $^nJ_{CC}$ and Δ^nJ_{CC} have been reproduced by theoretical *ab initio* MCSCF linear response calculations, where already a small multireference expansion is seen to be able to provide reasonable results. However, the convergence with electron correlation of the dominating mechanisms involving the Fermi contact interaction is slow. The theoretical results for Δ^nJ_{CC} approach from above (in magnitude) the experimental ones and provide likely upper bounds to them. While the one-bond coupling anisotropy is well converged, the disagreement with experiment is larger in the two- and three-bond couplings, the former in particular. Semiempirical methods, whose results have previously been reported in the literature, are found to perform quite well in comparison with *ab initio* calculations for the CC couplings of benzene. The remarkable computational effort needed in calculating spin−spin coupling tensors for molecules the size of benzene by the MCSCF linear response method calls for other first principles approaches. The density-functional theory appears to offer one practical solution which, however, needs to be implemented in a way that allows efficient calculation of all the different contributions to **J** to also enable evaluation of the corresponding anisotropies. Finally, this work shows that the anisotropic contributions in the experimental D_{CC} couplings are small; the $|(1/2)J^{aniso}|$ is always less than 2% of the corresponding $|D^{exp}|$. In particular, for the *ortho* D_{CC}, which is the coupling detectable for liquid crystal molecules in mesophases, $|J^{aniso}/2D^{exp}|$ is only on the order of 0.5%. Consequently, no large error is made when D_{CC} couplings are utilized for the determination of structure and ordering of liquid crystals containing phenyl rings.

Acknowledgment. The authors are grateful to the Academy of Finland for financial support. We also express our gratitude to the Finnish Cultural Foundation (J.K.) and the Jenny and Antti Wihuri (J.V.) and Vilho, Yrjö and Kalle Väisälä (J.V.) Funds for grants. Kenneth Ruud, University of Oslo, is thanked for access to the DALTON code and useful discussions. Professor Reino Laatikainen and Matthias Niemitz, University of Kuopio, are thanked for access to a late version of PERCH and informative discussions. Computational resources were supplied by the Center for Scientific Computing, Espoo, Finland.

Supporting Information Available: Tables corresponding to Table 6 but for ZLI 1167 and Phase 4 liquid crystal solvents (2 pages). See any current masthead page for ordering and Internet access instructions.

JA961263P